To appear in "Magnetic Coupling between the Interior and the Atmosphere of the Sun", eds. S. S. Hasan and R. J. Rutten, Astrophysics and Space Science Proceedings, Springer-Verlag, Heidelberg, Berlin, 2009.

A Topology for the Penumbral Magnetic Fields

J. Sánchez Almeida

Instituto de Astrofísica de Canarias, La Laguna, Tenerife, Spain

Summary. We describe a scenario for the topology of the magnetic field in penumbrae that accounts for recent observations showing upflows, downflows, and reverse magnetic polarities. According to our conjecture, short narrow magnetic loops fill the penumbral photosphere. Flows along these arched field lines are responsible for both the Evershed effect and the convective transport. This scenario seems to be qualitatively consistent with most existing observations, including the dark cores in penumbral filaments reported by Scharmer et al. Each bright filament with dark core would be a system of two paired convective rolls with the dark core tracing the common lane where the plasma sinks down. The magnetic loops would have a hot footpoint in one of the bright filament and a cold footpoint in the dark core. The scenario fits in most of our theoretical prejudices (siphon flows along field lines, presence of overturning convection, drag of field lines by downdrafts, etc). If the conjecture turns out to be correct, the mild upward and downward velocities observed in penumbrae must increase upon improving the resolution. This and other observational tests to support or disprove the scenario are put forward.

1 Introduction

We are celebrating the centenary of the discovery by John Evershed (1909) of the effect now bearing his name. Photospheric spectral lines in sunspots are systematically shifted toward the red in the limb-side penumbra, and toward the blue in the center-side penumbra. A hundred years have passed and, despite the remarkably large number of works on the Evershed effect[1], we still ignore how and why these line shifts are produced (see, e.g., the review paper by Thomas & Weiss 2004). Thus, the Evershed effect is among the oldest unsolved problems in astronomy. Although its study has never disappeared from the specialized literature, the Evershed effect has undergone a recent

[1] The NASA Astrophysics Data System provides more than fourteen hundred papers under the keyword *penumbra*, seventy of them published during the last year.

revival triggered by the advent of new instrumentation (Scharmer et al. 2002; Kosugi et al. 2007), original theoretical ideas (Weiss et al. 2004; Spruit & Scharmer 2006), as well as realistic numerical simulations (Heinemann et al. 2007; Rempel et al. 2008). Unfortunately, this renewed interest has not come together with a renewal of the diagnostic techniques, i.e., the methods and procedures that allow us to infer physical properties from observed images and spectra. Often implicitly, the observers assume the physical properties to be constant in the resolution element, a working hypothesis clearly at odds with the observations. Spectral line asymmetries show up even with our best spatial resolution (Ichimoto et al. 2007a; Sánchez Almeida et al. 2007, § 2). This lack of enough resolution is not secondary. The nature of the Evershed flow has remained elusive so far because we have been unable to isolate and identify the physical processes responsible for the line shifts. Different measurements provide different ill-defined averages of the same unresolved underlaying structure, thus preventing simple interpretations and yielding the problems of consistency that plague the Evershed literature (e.g., non-parallelism between magnetic field lines and flows, Arena et al. 1990; violation of the conservation of magnetic flux, Sánchez Almeida 1998; non-parallelism between continuum filaments and magnetic field lines, Kàlmàn 1991).

Understanding the observed spectral line asymmetries complicates our analysis but, in reward, the asymmetries provide a unique diagnostic tool. They arise from sub-pixel variations of the magnetic fields and flows, therefore, by modeling and interpretation of asymmetries, one can get a handle on the unresolved structure. Although indirectly, such modelling allows us to surpass the limitations imposed by the finite resolution. The idea has tradition in penumbral research, starting from the discovery of the asymmetries almost fifty years ago (e.g., Bumba 1960; Grigorjev & Katz 1972). Sánchez Almeida (2005, hereinafter SA05) exploits the tool in a systematic study that encompasses a full round sunspot. The unresolved components found by SA05 inspire the topology for the penumbral magnetic fields proposed here. According to SA05, the asymmetries of the Stokes profiles[2] can be *quantitatively* explained if magnetic fields having a polarity opposite to the sunspot main polarity are common throughout the penumbra. The reverse polarity holds intense magnetic field aligned flows which, consequently, are directed downward. Counter-intuitive as it may be, the presence of such ubiquitous strongly redshifted reverse polarity has been directly observed with the satellite HINODE (Ichimoto et al. 2007a). This new finding supports the original SA05 results, providing credibility to the constraints that they impose on the magnetic fields and mass flows. The existence of such ubiquitous return of magnetic flux, to-

[2] We use Stokes parameters to characterize the polarization; I for the intensity, Q and U for the two independent types of linear polarization, and V for the circular polarization. The Stokes profiles are representations of I, Q, U and V versus wavelength for a particular spectral line. They follow well defined symmetries when the atmosphere has constant magnetic field and velocity (see, e.g., Sánchez Almeida et al. 1996).

gether with a number of selected results from the literature, are assembled here to offer a plausible scenario for the penumbral magnetic field topology. Such exercise to piece together and synthesize information from different sources is confessedly speculative. It will not lead to a self-consistent MHD model for the penumbral structure. However, the exercise is worthwhile for a number of reasons. First, the compilation of observational results and theoretical arguments in § 2 provides a unique brief-yet-restrictive list of constraints to be satisfied by any explanation of the Evershed effect deserving such name. This reference compilation will be useful even if the proposed magnetic topology turns out to be incorrect. Second, we will show how the presence of a reverse polarity is qualitatively consistent with all existing observations, including unobvious cases. Third, despite the amount of observational and theoretical papers on penumbrae, our understanding of the Evershed phenomenon is far from satisfactory. The solution to the riddle cannot be trivial, and it may require interpreting the observations with an alternative twist. Unconventional proposals are needed, and here we explore some of the possibilities. Finally, the proposal may help inspiring MHD numerical modelers.

The work is structured as follows: it begins by summarizing a number of observations to constrain the topology of the magnetic field and velocity in penumbrae (§ 2). These observational results leave an important loose end. The reverse polarity found by Ichimoto et al. (2007a) does not show up in high spatial resolution observations with the Swedish Solar Telescope (SST; Langhans et al. 2005, 2007). § 3 explains how the apparent inconsistency goes away if the dark cores in penumbral filaments found by Scharmer et al. (2002) correspond to the strongly redshifted reverse polarity regions spotted by HINODE. Once the difficulty has been cleared up, the actual scenario for the magnetic field topology is put forward in § 4. Its predictions are qualitatively compared with observations in § 5. Similarities and differences between this scenario and existing models for the penumbral structure and the Evershed flow are analyzed in § 6, where we also suggest observational tests to confirm or disprove our conjecture.

2 Constraints on the penumbral structure

The bibliography on the magnetic structure of penumbrae is too extensive to be condensed in a few pages (see footnote # 1). We refrain from giving an overview, and those readers interested in a more formal review should refer to, e.g., Schmidt (1991), Thomas & Weiss (1992), Solanki (2003), Bellot Rubio (2004), or Thomas & Weiss (2004). Only the selected references that provide a framework for our proposal are introduced and discussed here. They include SA05 and Ichimoto et al. (2007a). Most of them are pure observational results, but several items involve theoretical arguments as well. The selection is obviously biased in the sense that some observations often bypassed are

emphasized here, and vice versa. However, to the best of our knowledge, no potentially important constraint has been excluded.

1. The best penumbral images have a resolution of the order $0\farcs12$ (or 90 km on the Sun). They show many features at the resolution limit implying the existence of unresolved substructure. For example, the power spectrum of the penumbral images has signal down to the instrumental cutoff (Rouppe van der Voort et al. 2004), and the width of the narrower penumbral filaments is set by the resolution of the observation (Scharmer et al. 2002; see also Fig. 1). This interpretation of the current observations should not be misunderstood. The penumbrae have structures of all sizes starting with the penumbra as a whole. However, the observations show that much of its observed structure is at the resolution set by the present technical limitations and, therefore, it is expected to be unresolved. This impression is corroborated by the presence of spectral line asymmetries as discussed in item 11.
2. The best penumbral images show *dark cores in penumbral filaments* (Scharmer et al. 2002). We prefer to describe them as dark filaments outlined by bright plasma. This description also provides a fair account of the actual observation (Fig. 1), but it emphasizes the role of the dark core. Actually, dark cores without a bright side are common, and the cores seldom emanate from a bright point (Fig. 1). The widths of the dark core and its bright boundaries remain unresolved, although the set formed by a dark core sandwiched between two bright filaments spans some 150-180 km across.
3. There is a local correlation between penumbral brightness and Doppler shift, so that bright features are blueshifted with respect to dark features (Beckers & Schröter 1969; Sánchez Almeida et al. 1993, 2007; Johannesson 1993; Schmidt & Schlichenmaier 2000). The correlation maintains the same sign in the limb-side penumbra and the center-side penumbra, a property invoked by Beckers & Schröter (1969) to conclude that it is produced by vertical motions. A positive correlation between vertical velocity and intensity is characteristic of the non-magnetic granulation. The fact that the same correlation also exists in penumbrae suggests a common origin for the two phenomena, namely, convection.
4. The limb-side and center-side parts of a penumbra are slightly darker than the rest, an observational fact indicating that the bright penumbral filaments are elevated with respect to the dark ones (Schmidt & Fritz 2004). The behavior seems to continue down to the smallest structures. Dark cores are best seeing where the low resolution penumbra is darkest according to Schmidt & Fritz (2004), i.e., along the center-to-limb direction (e.g., Langhans et al. 2007; Ichimoto et al. 2007b). The two observations are probably connected, suggesting that dark cores are depressed with respect to their bright sides.

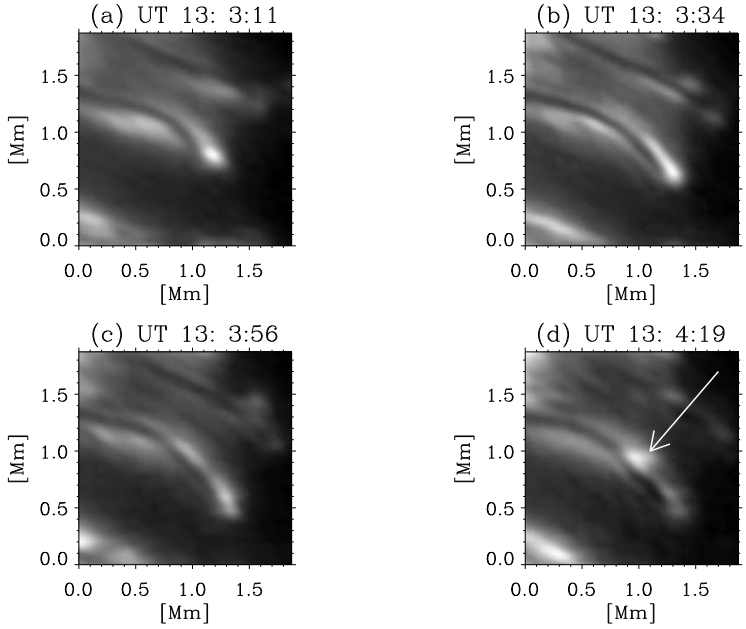

Fig. 1. Time evolution of one of the *dark cores in penumbral filaments* discovered by Scharmer et al. (2002). (The UT of observation is marked on top of each snapshot.) Note that one of the bright sides is partly missing in (c) and (d). Note also that the bright points are not on the dark filament but in a side. These two properties are common. The arrow indicates the emergence of a new bright point in a side of the pre-existing dark filament. Note the narrowness of the bright filaments, and their large aspect ratio (length over width). The spatial scales are in Mm, and the angular resolution of the image is of the order of 0.09 Mm.

5. There is a local correlation between magnetic field inclination and horizontal velocity. The largest velocities are associated with the more horizontal fields (e.g., Title et al. 1993; Stanchfield et al. 1997).
6. The large horizontal motions occur in the dark penumbral filaments (e.g., Rüedi et al. 1999; Penn et al. 2003; Sánchez Almeida et al. 2007). This trend continues down to the dark cores in penumbral filaments (Langhans et al. 2005, 2007).
7. The observations on the correlation between magnetic field strength and brightness are contradictory. Some authors find the strongest field strengths associated with the darkest regions, and vice versa (c.f. Beckers & Schröter 1969 and Hofmann et al. 1994). What seems to be clear is the reduced circular polarization signal existing in dark cores, which is commonly interpreted as a reduced field strength (Langhans et al. 2005, 2007). We show in § 3 that such dimming of the circular polarization ad-

mits a totally different interpretation, consistent with an increase of field strength in dark cores.

8. Theoretical arguments indicate that the convective roll pattern should be the mode of convection for nearly horizontal magnetic fields (Danielson 1961; Hurlburt et al. 2000). The rolls have their axes along the magnetic field lines. Unfortunately, this is not what results from recent numerical simulations of magneto-convection in strong highly inclined magnetic fields (Heinemann et al. 2007; Rempel et al. 2008). Here the convection takes place as field-free plasma intrusions in a strong field background, resembling the gappy penumbra model by Spruit & Scharmer (2006). However, these numerical simulations many not be realistic enough. They are the first to come in a series trying to reduce the artificial diffusivities employed by the numerical schemes. It is unclear whether such evolution will maintain the modes of convection. Moreover, even the present simulations hint at the existence of a convective roll pattern.
9. The stable sunspots are surrounded by a large annular convection cell called moat (Sheeley 1972). The moat presents an outflow which, contrarily to the commonly held opinion, has both radial and tangential velocities (Title 2003, private communication; Bonet et al. 2005). The tangential component is well organized so that it sweeps the plasma toward radial channels, creating a velocity pattern that resembles the convective rolls by Danielson (1961). Compare Fig. 7 in Bonet et al. (2005) or Fig. 11 in Bovelet & Wiehr (2003) with the rolls in Fig. 9a of García de la Rosa (1987).
10. The magnetic field lines can be dragged by the downdrafts of the granulation. Termed as *flux pumping* mechanism, this drag is modeled and studied by Weiss et al. (2004) and Brummell et al. (2008) to show that the vigorous sinking plumes of the granulation and mesogranulation easily pumps down magnetic fluxtubes outside the penumbra. It is conceivable that the same pumping by sinking plasma also operates within the magnetized penumbra.
11. The polarization of the spectral lines emerging from any sunspot has asymmetries and, consequently, it requires several unresolved velocities and magnetic fields to be produced (Bumba 1960; Grigorjev & Katz 1972; Golovko 1974; Sánchez Almeida & Lites 1992). The asymmetries show up even with the best spatial resolution achieved nowadays (150 km – 250 km; Sánchez Almeida et al. 2007, Ichimoto et al. 2007a). Furthermore, part of the substructure producing asymmetries will never be resolved directly because it occurs along the line-of-sight (LOS). The spectral lines create net circular polarization (NCP), i.e., the asymmetry of the Stokes V profiles is such that the integrated circular polarization of any typical spectral line is not zero. NCP can only be produced by gradients along the LOS and, therefore, within a range of heights smaller that the region where the lines are formed (say, 100 km). The NCP follows several general rules found by Illing et al. (1974a,b) and Makita (1986). Explaining them requires large

gradients of magnetic field inclination along the LOS (Sánchez Almeida & Lites 1992). The gradients can be produced by the discontinuities occurring at the boundary of relatively large magnetic fluxtubes embedded in a background (Solanki & Montavon 1993), or as the cumulative effect of several smaller optically thin structures with varied magnetic field inclinations (Sánchez Almeida et al. 1996).

12. The sunspots seem to show upward motions in the inner penumbra and downward motions in the outer penumbra (e.g., Rimmele 1995; Schlichenmaier & Schmidt 2000; Bellot Rubio et al. 2003; Tritschler et al. 2004). However, this velocity pattern is inferred assuming uniform velocities in the resolution elements, an hypothesis inconsistent with observations (items 1 and 11).
13. Using a MISMA[3] framework, SA05 carries out a systematic fit of all Stokes profiles observed with $1''$-resolution in a medium sized sunspot. Line asymmetries and NCP are reproduced (item 11). The resulting semi-empirical model sunspot provides both the large scale magnetic structure, as well as the small scale properties of the micro-structure. On top of a regular large scale behavior, the inferred small scale structure of the magnetic fields and flows is novel and unexpected. Some 30% of the volume is occupied by magnetic field lines that return to the sub-photosphere within the penumbral boundary. Mass flows are aligned with magnetic field lines, therefore, the field lines with the main sunspot polarity transport mass upward, whereas the reverse polarity is associated with high speed flows returning to the solar interior. This return of magnetic flux and mass toward the solar interior occurs throughout the penumbra, as opposed to previous claims of bending over and return at the penumbral border or beyond (item 12). The observed magnetic field strength difference between field lines pointing up and down can drive a siphon flow with the magnitude and sense of the Evershed flow. Within observational uncertainties, the mass transported upward is identical to the mass going downward.
14. The bright penumbral filaments are too long to trace individual streams of hot plasma. The original argument dates back to Danielson (1960), but here we recreate a recent account by Schlichenmaier et al. (1999). They estimate the length of a bright filament produced by hot plasma flowing along a magnetic fluxtube. The plasma cools down as it radiates away and so, eventually, the fluxtube becomes dark and transparent. An isolated loop would have a bright head whose length l is approximately set by the cooling time of the emerging plasma t_c times the velocity of the mass flow along the field lines U,

$$l \approx U t_c. \tag{1}$$

[3] The acronym MISMA stands for MIcro-Structured Magnetic Atmosphere, and it was coined by Sánchez Almeida et al. (1996) to describe magnetic atmospheres having optically-thin substructure.

The cooling time depends on the diameter of the tube d, so that the thinner the tube the faster the cooling. For reasonable values of the Evershed flow speed (U$\approx$ 5 km s^{-1}), and using the cooling time worked out by Schlichenmaier et al. (1999), the aspect ratio of the hot footpoint turns out to be of the order of one for a wide range of fluxtube diameters, i.e.,

$$l/d \approx 0.8\ (d/200\ \mathrm{km})^{0.5}. \quad (2)$$

Filaments must have $l/d >> 1$, and so, a hot plasma stream will show up as a bright knot rather than as a filament. In other words, the cooling of hot plasma moving along field lines cannot give rise to the kind of observed filaments (see Fig. 1). If arrays of hot plasma streams form the filaments, they must be arranged with their hot and cold footpoints aligned to give rise to the observed structures.

15. HINODE magnetograms of penumbrae obtained in the far wings of Fe I λ6302.5 Å show a redshifted magnetic component with a polarity opposite to the main sunspot polarity (Fig. 4 in Ichimoto et al. 2007a). The patches of opposite polarity are scattered throughout the penumbra. In addition, this reverse polarity is associated with extremely asymmetric Stokes V profiles having three lobes (Ichimoto et al. 2007a, Fig. 5, and Ichimoto 2008, private communication). These asymmetric profiles are known in the traditional literature as cross-over effect, a term used along the paper.

3 Model MISMA for penumbral filaments with dark core

The set of constraints summarized in § 2 leave an important loose end. The reverse polarity predicted by SA05 (item 13) and found by Ichimoto et al. (2007a, item 15) does not show up in SST magnetograms (Langhans et al. 2005, 2007, and § 1). This fact poses a serious problem since SST has twice HINODE spatial resolution and, therefore, it should be simpler for SST to detect mixed polarities. Here we show how HINODE and SST observations can be naturally understood within the two component model MISMA by SA05, provided that the dark cores are associated with an enhanced contribution of the reverse polarity.

According to SA05, the component that contains most of the mass in each resolution element has the polarity of the sunspot, and bears mild magnetic-field-aligned mass flows. It is usually combined with a minor component of opposite polarity and having large velocities. In 1″-resolution observations, the outcoming light is systematically dominated by the major component, and the resulting Stokes profiles have rather regular shapes. An exception occurs in the so-called *apparent neutral line*, where the cross-over effect was discovered (see Sánchez Almeida & Lites 1992, and references therein). At the neutral line the mean magnetic field vector is perpendicular to the LOS, and the contribution of the major component almost disappears due to projection effects.

The improvement of angular resolution augments the chances of finding the minor component in excess, allowing the opposite polarity to show up. In order to illustrate the effect, several randomly chosen model MISMAs in SA05 were modified by increasing the fraction of atmosphere occupied by the minor component. One example is shown in Fig. 2. The resulting Stokes I, Q and V profiles of Fe I λ6302.5 Å are represented as solid lines in Figs. 2a, 2b and 2c, respectively. They model a point in the limb-side penumbra at $\mu = 0.95$ (18° heliocentric angle). Note how Stokes I is redshifted and deformed, and how Stokes V shows the cross-over effect. Consequently, the improvement of spatial resolution with respect to traditional earth-based spectro-polarimetric observations naturally explains the abundance of cross-over Stokes V profiles found by HINODE. Figures 2a, 2b, and 2c also show the case where the major component dominates (the dashed line). The strong asymmetries have disappeared, rendering Stokes V with antisymmetric shape and the sign of the dominant polarity. The magnetic field vector and the flows are identical in the two sets of Stokes profiles (Figs. 2e and 2f), although, we have globally decreased the temperature of the atmosphere giving rise to the asymmetric profiles to mimic dark features (see the Stokes I continua in Fig. 2a).

Understanding HINODE observations in terms of MISMAs also explains the lack of reverse polarity in SST magnetograms. Stokes V in reverse polarity regions shows cross-over effect (Fig. 5 in Ichimoto et al. 2007a, and Ichimoto 2008, private communication), i.e., it presents two polarities depending on the sampled wavelength. It has the main sunspot polarity near line center, whereas the polarity is reversed in the far red wing (see the solid line in Fig. 2c). SST magnetograms are taken at line center (±50 mÅ), which explains why the reverse polarity does not show up. A significant reduction of the Stokes V signal occurs, though. Such reduction automatically explains the observed weakening of magnetic signals in dark cores (item 7 in § 2), provided that the dark cores are associated with an enhancement of the opposite polarity, i.e., if the cross-over profiles are produced in the dark cores. We have constructed images, magnetograms, and dopplergrams of a (naïve) model dark-cored filament that illustrate the idea. The filament is formed by a uniform 100 km wide dark strip, representing the dark core, bounded by two bright strips of the same width, representing the bright sides. The Stokes profiles of the dark core have been taken as the solid lines in Figs. 2a and 2c, whereas the bright sides are modelled as the dashed lines in the same figures. The color filters employed by Langhans et al. (2005, 2007) are approximated by Gaussian functions of 80 mÅ FWHM, and shifted ±50 mÅ from the line center (see the dotted lines in Fig. 2a). The magnetogram signals are computed from the profiles as

$$M = \int V(\lambda) f(\lambda - \Delta\lambda)\, \mathrm{d}\lambda \Big/ \int I(\lambda) f(\lambda - \Delta\lambda)\, \mathrm{d}\lambda, \tag{3}$$

with $f(\lambda)$ the transmission curve of the filter and $\Delta\lambda = -50$ mÅ. Similarly, the Doppler signals are given by

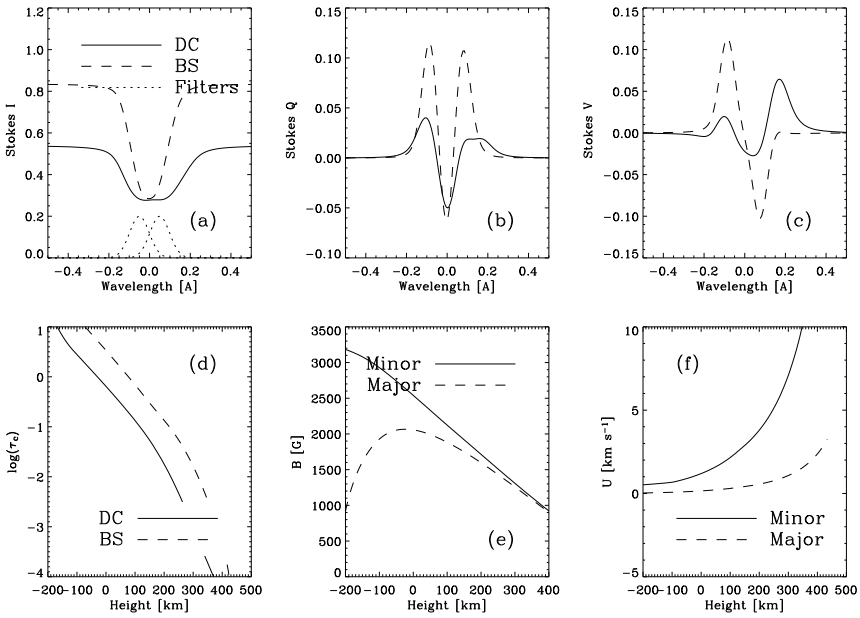

Fig. 2. (a) Stokes I profiles in one of the representative model MISMAs in SA05, which has been slightly modified to represent a dark core (the solid line), and its bright sides (the dashed line). They are normalized to the quiet Sun continuum intensity. (b) Stokes Q profiles. (c) Stokes V profiles. (d) Continuum optical depth τ_c vs height in the atmosphere for the dark core and the bright sides, as indicated in the inset. (e) Magnetic field strength vs height for the two magnetic components of the model MISMA. They are identical for the dark core and the bright sides. (f) Velocities along the magnetic field lines for the two magnetic components of the model MISMA. They are identical for the dark core and the bright sides.

$$D = \int I(\lambda)[f(\lambda-\Delta\lambda)-f(\lambda+\Delta\lambda)]\,\mathrm{d}\lambda \Big/ \int I(\lambda)[f(\lambda-\Delta\lambda)+f(\lambda+\Delta\lambda)]\,\mathrm{d}\lambda, \tag{4}$$

but here we employ the Stokes I profile of the non-magnetic line used by Langhans et al. (2007; i.e., Fe I λ5576 Å). The signs of M and D ensure $M > 0$ for the main polarity of the sunspot, and also $D > 0$ for redshifted profiles. The continuum intensity has been taken as I at -0.4 Å from the line center. The continuum image of this model filament is shown in Fig. 3, with the dark core and the bright sides marked as DC and BS, respectively. The dopplergram and the magnetogram are also included in the same figure. The dark background in all images indicates the level corresponding to no signal. In agreement with Langhans et al. observations, the filament shows redshifts ($D > 0$), which are enhanced in the dark core. In agreement with Langhans et al., the filament shows the main polarity of the sunspot ($M > 0$),

with the signal strongly reduced in the dark core. Figure 3, bottom, includes the magnetogram to be observed at the far red wing ($\Delta\lambda = 200\,\mathrm{m\AA}$). The dark core now shows the reversed polarity ($M < 0$), whereas the bright sides still maintain the main polarity with an extremely weak signal. This specific prediction of the modeling is liable for direct observational test (§ 6).

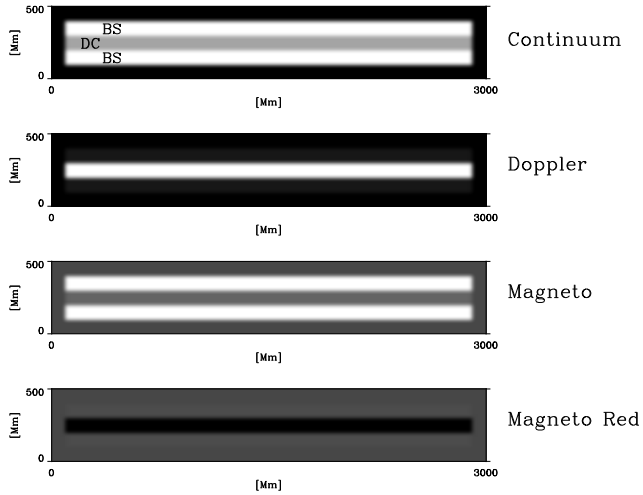

Fig. 3. Schematic modeling of SST observations of penumbral filaments by Langhans et al. (2005, 2007). A dark core (DC) surrounded by two bright sides (BS) is located in the limb-side penumbra of a sunspot at $\mu = 0.95$ (18° heliocentric angle). The three top images show a continuum image, a dopplergram, and a magnetogram, as labelled. The convention is such that both the sunspot main polarity and a redshift produce positive signals. The dark background in all images has been included for reference, and it represents signal equals zero. The fourth image (`Magneto Red`) corresponds to a magnetogram in the far red wing of Fe I λ6302.5 Å, and it reveals a dark core with a polarity opposite to the sunspot main polarity. The continuum image and the dopplergram have been scaled from zero (black) to maximum (white). The scaling of the two magnetograms is the same, so that their signals can be compared directly.

Two final remarks are in order. First, the magnetogram signal in the dark core is much weaker than in the bright sides, despite the fact that the (average) magnetic field strength is larger in the core (see Fig. 2e, keeping in mind that the minor component dominates). Second, the model dark core is depressed with respect to the bright sides. Figure 2d shows the continuum optical depth τ_c as a function of the height in the atmosphere. When the two atmospheres are in lateral pressure balance, the layer $\tau_c = 1$ of the dark core is shifted by some 100 km downward with respect to the same layer in the bright sides. The depression of the observed layers in the dark core is produced by two effects;

the decrease of density associated with the increase of magnetic pressure (e.g., Spruit 1976), and the decrease of opacity associated with the reduction of temperature (e.g., Stix 1991).

4 Scenario for the small-scale structure of the penumbra

Attending to the constraints presented in § 2, penumbrae may be made out of short narrow shallow magnetic loops which often return under the photosphere within the sunspot boundary (Fig. 4). One of the footpoints is hotter than the other (Fig. 5). The matter emerges in the hot footpoint, radiates away, cools down, and returns through the cold footpoint. The ascending plasma is hot, dense, and slowly moving. The descending plasma is cold, tenuous, and fast moving. The motions along magnetic field lines are driven by magnetic field strength differences between the two footpoints, as required by the siphon flow mechanism.

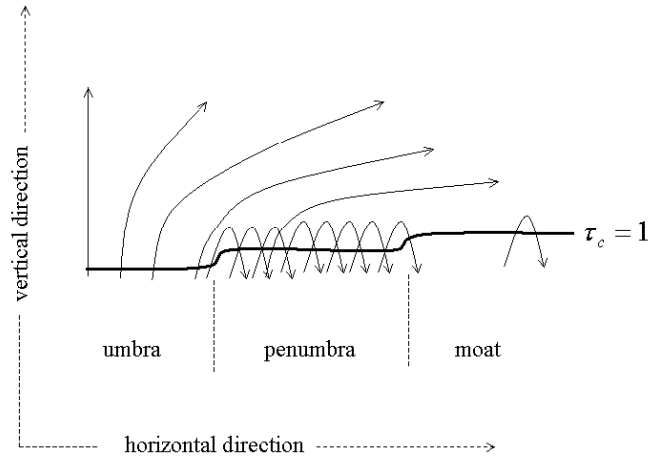

Fig. 4. Cartoon sketching the scenario for the penumbral magnetic field topology put forward in the paper. Magnetic field lines, represented as solid lines with arrow heads, return under the photosphere in the entire penumbra. The symbol τ_c stands for the continuum optical depth so that the thick solid line marked as $\tau_c = 1$ represents the base of the photosphere.

In addition to holding large velocities along field lines, the cold footpoint of each loop sinks down in a slow motion across field lines. In non-magnetic convection, upflows are driven through mass conservation by displacing warm material around the downdrafts (Stein & Nordlund 1998; Rast 2003). The

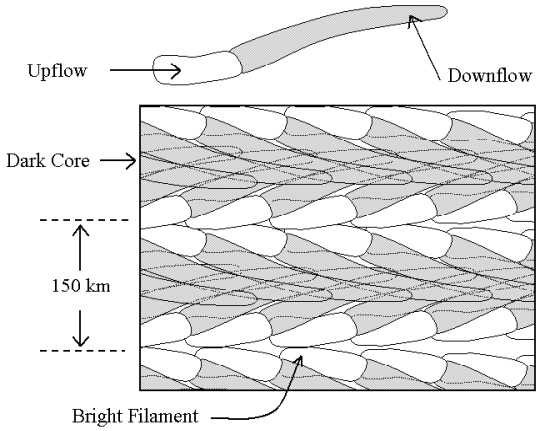

Fig. 5. A view from above of a small portion of penumbra (see the scale on the left hand side of the cartoon). Small magnetic loops like the one on top of the figure are averaged in our resolution element (the rectangle). They are so thin that various loops overlap along the LOS. The loops are arranged with the downflowing footpoints aligned forming a dark core. The hot upflows feeding a dark core give rise to two bright filaments. The Evershed flow is directed along the field lines toward the right.

uprising hot material tends to emerge next to the downflows. If the same mechanism holds in penumbrae, the sinking of cold footpoints induces a rise of the hot footpoints physically connected to them, producing a backward displacement of the visible part of the loops (see Fig. 6). The sink of the cold footpoints could be forced by the drag of downdrafts in subphotospheric layers, in a magnetically modified version of the mechanism discussed in item 10 of § 2.

The properties of the loops (length, width, speed, and so on) should change with the position on the penumbra, but they are always narrow and so tending to be optically-thin across field lines. One does not detect individual loops but assembles of them interleaved along the LOS. The cold legs of many different loops should be identified with the dark cores found by Scharmer et al. (2002); compare Figs. 1 and 5. The upflows of many loops account for be bright penumbral filaments. In this scenario, magnetic field lines are not exactly aligned with the penumbral bright and dark filaments, but the field lines diverge from the bright filaments and converge toward the dark filaments. The mean field is radial, though.

According to our scenario, bright penumbral filaments are associated with fields having the polarity of the sunspot, mild upflows, and relatively low field strengths. On the contrary, dark filaments are associated with fields whose

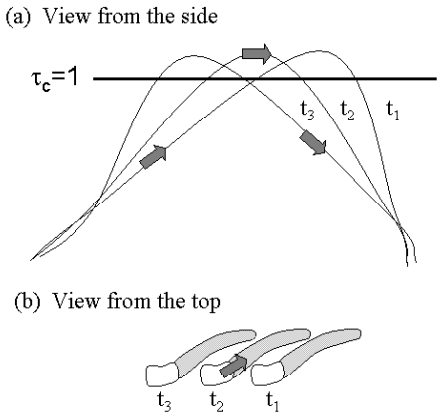

Fig. 6. Cartoon showing the time evolution of a single magnetic field line, with $t_1 < t_2 < t_3$ (the thin solid lines). (a) View from the side, with the vertical direction pointing upward. The thick solid line corresponds to base of the photosphere (continuum optical depth equals one). The Evershed flow is directed to the right. The thick arrows represent a parcel of fluid with the tip pointing in the direction of the plasma motion. (b) View from above of the same three instants. (Compare with Fig. 5, showing many field lines at a given time.) It only shows the fluid parcel at t_2 since it remains below the photosphere at t_1 and t_3.

polarity tends to be opposite to the sunspot polarity, have intense flows, high field strength, and they are more transparent than the bright filaments.

5 Qualitative comparison with observations

As we will discuss here, the scenario proposed in § 4 fits in the observations in § 2. Our model penumbra is formed by narrow loops whose length is typically smaller than the penumbral size (Fig. 4), and whose width is not spatially resolved. The smallness of the physical scales is in agreement with items 1 and 11. (These and the rest of numbers refer to the labels in § 2.) Magnetic field lines bend over and return under the photosphere over the entire penumbra, as required by items 13 and 15. The loops have a hot footpoint with upward motion and a cold footpoint with downward motion, in agreement with the local correlation between brightness and upward velocity observed in penumbrae (item 3). The downflows are expected to be faster than the upflows since they are accelerated by the magnetic field strength difference between the two footpoints, an image that fits in well the observations showing the largest velocities to be associated with the dark penumbral components (item 6).

We identify the dark cores found by Scharmer et al. (2002, item 2) with cold footpoints of many loops, as sketched in Fig. 5. Dark cores trace downdrafts engulfing cold footpoints (item 10). The bright filaments around the dark cores would be naturally explained by the presence of the downflows, as it happens with the enhanced brightness at the borders of the granules in non-magnetic convection. Mass conservation induces an upflow of hot material around the downdrafts (Rast 1995, 2003; Stein & Nordlund 1998). The same mechanism would produce the upraise of hot (magnetized) material around the dark cores, forming two bright filaments outlining each core (item 2; Fig. 1). The hot magnetized material would eventually cool down and sink into the dark core to re-start the process. In other words, a dark core would be the downdraft of two paired convective rolls, resembling those proposed long ago by Danielson (item 9). In this case, however, the magnetic field lines are not exactly horizontal, and the plasma has a large velocity component along the field lines. Note that these hypothetical convective rolls reproduce the expected mode of convective transport in highly inclined magnetic fields (see item 8, including the comment on the recent numerical simulations of penumbrae which seem to disfavor this mode). Moreover, a pattern of motions similar to these convective rolls occurs in the moat surrounding the sunspot (item 9), and it is conceivable that it continues within the sunspot.

The existence of small scale convective upflows and downflows does not contradict the systematic upward motions in the inner penumbra and downward motions in the outer penumbra found by various authors (see item 12). Most observational techniques employed so far assume uniform velocities in the resolution element. When spatially unresolved upflows and downflows are interpreted as a single resolved component, the measured velocity corresponds to an ill-defined mean of the actual velocities. The contribution of upflows and downflows to such mean is not proportional to the mass going up and down. It depends on the physical properties of the upflows and downflows, as well as on the method employed to measure. The mean vertical flux of mass inferred by SA05 is zero (item 13), however the local averages are biased[4], showing net upflows in the inner penumbra and net downflows in the outer penumbra, in agreement with item 12.

Our scenario with overlaying loops of various velocities and inclinations accounts for the observed Stokes asymmetries, including the rules for the NCP mentioned in item 11.

The bright filaments are more opaque than the dark cores (§ 3), and they tend to block the light coming from the dark cores when the filaments are observed sideways. This depression of the dark cores explains why they are elusive in the penumbra perpendicular to the center-to-limb direction, as well

[4] The effect is similar to the convective blueshift of the spectral lines formed in the granulation, whose existence does not imply a net uplifting of the quiet photosphere.

as why penumbrae are slightly darker in the line along the center-to-limb direction (item 4).

The length of the bright filaments is not set by the cooling time of individual fluxtubes, which avoids the difficulty posed in item 14. It is given by the length of the dark core.

Does the model account for the penumbral radiative flux? The radiative flux emanating from penumbrae F is some 75% of the flux in the quiet Sun. In order to balance this loss with energy transported by convection, the vertical velocity U_z must satisfy (e.g., Spruit 1987; Stein & Nordlund 1998),

$$U_z \approx F/(\rho\alpha\epsilon) \approx 1 \text{ km s}^{-1}, \tag{5}$$

with ρ the density, α fraction of atmospheric volume occupied by upward motions, and ϵ the energy per unit mass to be radiated away. Since the physical conditions in penumbrae are similar to those of the quiet Sun, the U_z accounting for F must be similar too, rendering the speed in the right-hand-side of equation (5). Unfortunately, the observed upward vertical velocities are one order of magnitude smaller than the requirement set by equation (5)[5] (items 3 and 13). The discrepancy can be explained if an observational bias underestimates the true velocities. Such bias is to be expected because the velocity structure remains unresolved (items 1 and 11). Removing the bias involves resolving the structure both along and across the LOS, in particular, the cross-over effect Stokes V profiles associated with the reverse polarity must be properly interpreted to retrieve realistic velocities.

Why does the low-density plasma of the cold footpoints sink rather than float? We have been arguing by analogy with the non-magnetic convection, where the (negative) buoyancy forces in the intergranular lanes drive the sinking of cold plasma, and the rising of hot material around it. The plasma tends to sink down due to its enhanced density as compared to the hot upwelling plasma. The scenario for the penumbral convection discussed above does not reproduce this particular aspect of the granular convection. The descending footpoint has reduced density as compared to the upflowing footpoint. The density in the descending leg is lower than in the ascending leg, and one may think that the descending plasma is buoyant. However, the density of the cold leg has to be compared to the local density in the downdraft, which can easily be larger than the downdraft density. Recall that the downdrafts have low temperature and high magnetic field strengths, two ingredients that naturally produce low densities in magneto-hydrostatic equilibrium (see, e.g., Sánchez Almeida 2001).

Why are the dark cores radially oriented? According to our conjecture, the dark cores are not tracing individual field lines. They are faults in the global structure of the sunspot where downflow motions are easier. Such

[5] This discrepancy between the required and observed velocities was used to discard the transport of energy by convection in penumbrae (Spruit 1987), leading to the concept of shallow penumbra by Schmidt et al. (1986).

discontinuities of the global magnetic structure would be favored if they are aligned with the mean magnetic field, as it happens with interchange instabilities (Parker 1975; Meyer et al. 1977; Jahn & Schmidt 1994). The dark cores would be oriented along the direction of the mean penumbral magnetic field.

6 Discussion and tests

We have described a penumbral magnetic field formed by short magnetic loops most of which return to the sub-photosphere within the sunspot boundary (Fig. 4). Matter flowing along magnetic field lines would give rise to the Evershed effect. This flow along field lines would also be responsible for the convective transport of heat in penumbrae. Cold downflows of many loops are aligned in a sort of lane of downdrafts whose observational counterpart would be the dark cores in penumbral filaments found by Scharmer et al. (2002). To some extent, the scenario resembles the convective rolls put forward by Danielson some 50 years ago, except that (a) the mass also flows along field lines, and (b) the mass may not re-emerge after submergence. It is also akin to the interchange convection (e.g., Schlichenmaier 2002), where flows along field lines transport heat from below and give rise to the Evershed effect phenomena. In our case, however, the upraise of the hot tubes is induced by the presence of downdrafts and the need to satisfy mass conservation (as in the non-magnetic granular convection). The submergence of the cool footpoints of the loops happening in the downdrafts may be due to flux pumping, as numerical models have shown to occur in the non-magnetic downdrafts outside penumbrae (Weiss et al. 2004). Our scenario also owes some properties to the siphon flow model (Meyer & Schmidt 1968; Thomas & Montesinos 1993). A gas pressure difference between the loop footpoints drives the flows, but this difference is set by the magnetic field strength difference between the hot and the cold penumbral structures, rather than from field strength differences between the penumbra and magnetic concentrations outside the sunspot. Finally, the model that emerges has features from the return flux model of Osherovich (1982), where the field lines forming umbra and penumbra differ because the former are open whereas the latter return to the photosphere. The return of magnetic flux is included in our scenario, except that the return of penumbral field lines occurs throughout the penumbra, rather than outside the sunspot border.

This scenario seems to be compatible with most observations existing in the literature, in particular, with the ubiquitous downflows and the reverse magnetic flux found by SA05 and Ichimoto et al. (2007a) (see § 5). However, two difficulties remain. First, the upflows and downflows measured so far are not fast enough to transport the radiative flux emerging from penumbrae (§ 5). Second, the reverse polarity does not show up in SST observations, which nevertheless provide the highest spatial resolution available at present (§ 3). We believe that the two difficulties are caused by our still insufficient resolution.

Solving the problem is not only a question of improving the resolution across the LOS (e.g., by enlarging the telescope diameter), but the resolution along the LOS seems to be critical. The finding by Ichimoto et al. (2007a) that the reverse polarity coincides with very asymmetric Stokes profiles with NCP strongly suggests that measuring the true velocities and polarities demands resolution along the LOS. In other words, the observed polarization cannot be correctly interpreted if one assumes the light to come from an atmosphere with uniform properties.

Several specific tests will allow us to confirm or falsify the scenario. (1) Diffraction limited high resolution spectro-polarimetry with 1-meter class telescopes must show a correlation between brightness and velocity with an amplitude of the order of 1 km s^{-1}. As we point out above, a pure brute force approach may not suffice to render the right amplitude, and modeling the observed asymmetries seems to be required. (2) SST magnetograms taken in the far red wing of Fe I 6302.5 Å must show dark cores with reverse polarity (§ 3). (3) The molecular spectra trace the cold penumbral component (e.g., Penn et al. 2003). They should show a global downflow of the order of 1 km s^{-1}, no matter the angular resolution of the observation. (4) Local correlation tracking techniques applied to sequences of penumbral images should reveal proper motions of bright features moving toward dark filaments. Such motions are masked by the tendency of the bright plasma to cool down and become dark. A global trend is to be expected, though. Such trend seems to be present in high resolution SST images (Márquez et al. 2006), although the result requires independent confirmation.

Acknowledgement. In a paper for non-specialists, Priest (2003) speculates *"Are the bright filaments doubly convective rolls with a dark core that are cooling and sinking?"* This question seems to advance the scenario advocated here. In addition, the scenario is sketched in an unpublished work by Sánchez Almeida (2004), and it is also mentioned in Sánchez Almeida (2006). Using arguments differing from those introduced here, Zakharov et al. (2008) have recently claimed evidence for convective rolls in penumbrae. The image in Fig. 1 is courtesy of the Institute for Solar Physics of the Royal Swedish Academy of Sciences, and it was obtained with the SST operated in the Spanish Observatorio del Roque de Los Muchachos (La Palma). The work has partly been funded by the Spanish Ministry of Science and Technology, project AYA2007-66502, as well as by the EC SOLAIRE Network (MTRN-CT-2006-035484). I thank the SOC of the Evershed centenary meeting for this opportunity to expound unconventional ideas.

References

Arena, P., Landi Degl'Innocenti, E., Noci, G. 1990, Solar Phys., 129, 259
Beckers, J. M. Schröter, E. H. 1969, Solar Phys., 10, 384
Bellot Rubio, L. R. 2004, Rev. Mod. Astron., 17, 21

Bellot Rubio, L. R., Balthasar, H., Collados, M., Schlichenmaier, R. 2003, A&A, 403, L47
Bonet, J. A., Márquez, I., Muller, R., Sobotka, M., Roudier, T. 2005, A&A, 430, 1089
Bovelet, B. Wiehr, E. 2003, A&A, 412, 249
Brummell, N. H., Tobias, S. M., Thomas, J. H., Weiss, N. O. 2008, ApJ, 686, 1454
Bumba, V. 1960, Izv. Crim. Astrophys. Obs., 23, 253
Danielson, R. E. 1960, AJ, 70, 343
Danielson, R. E. 1961, ApJ, 134, 289
Evershed, J. 1909, MNRAS, 69, 454
García de la Rosa, J. I. 1987, in The Role of Fine-Scale Magnetic Fields on the Structure of the Solar Atmosphere, eds. E.-H. Schröter, M. Váquez, & A. A. Wyller, Cambridge University Press, Cambridge, 140
Golovko, A. A. 1974, Solar Phys., 37, 113
Grigorjev, V. M. Katz, J. M. 1972, Solar Phys., 22, 119
Heinemann, T., Nordlund, Å., Scharmer, G. B., Spruit, H. C. 2007, ApJ, 669, 1390
Hofmann, J., Deubner, F.-L., Fleck, B., Schmidt, W. 1994, A&A, 284, 269
Hurlburt, N. E., Matthews, P. C., Rucklidge, A. M. 2000, Solar Phys., 192, 109
Ichimoto, K., Shine, R. A., Lites, B., et al. 2007a, PASJ, 59, 593
Ichimoto, K., Suematsu, Y., Tsuneta, S., et al. 2007b, Science, 318, 1597
Illing, R. M. E., Landman, D. A., Mickey, D. L. 1974a, A&A, 35, 327
Illing, R. M. E., Landman, D. A., Mickey, D. L. 1974b, A&A, 37, 97
Jahn, K. Schmidt, H. U. 1994, A&A, 290, 295
Johannesson, A. 1993, A&A, 273, 633
Kàlmàn, B. 1991, Solar Phys., 135, 299
Kosugi, T., Matsuzaki, K., Sakao, T., et al. 2007, Solar Phys., 243, 3
Langhans, K., Scharmer, G., Kiselman, D., Löfdahl, M., Berger, T. E. 2005, A&A, 436, 1087
Langhans, K., Scharmer, G. B., Kiselman, D., Löfdahl, M. G. 2007, A&A, 464, 763
Makita, M. 1986, Solar Phys., 106, 269
Márquez, I., Sánchez Almeida, J., Bonet, J. A. 2006, ApJ, 638, 553
Meyer, F. Schmidt, H. U. 1968, Mitteilungen der Astronomischen Gesellschaft Hamburg, 25, 194
Meyer, F., Schmidt, H. U., Weiss, N. O. 1977, MNRAS, 179, 741
Osherovich, V. A. 1982, Solar Phys., 77, 63
Parker, E. N. 1975, Solar Phys., 40, 291
Penn, M. J., Cao, W. D., Walton, S. R., Chapman, G. A., Livingston, W. 2003, ApJ, 590, L119
Priest, E. 2003, Physics World, 16(2), 19
Rüedi, I., Solanki, S. K., Keller, C. U. 1999, A&A, 348, L37
Rast, M. P. 1995, ApJ, 443, 863
Rast, M. P. 2003, ApJ, 597, 1200
Rempel, M., Schüssler, M., Knölker, M. 2008, ApJ, in press, astro-ph/0808.3294
Rimmele, T. R. 1995, ApJ, 445, 511
Rouppe van der Voort, L. H. M., Löfdahl, M. G., Kiselman, D., Scharmer, G. B. 2004, A&A, 414, 717
Sánchez Almeida, J. 1998, ApJ, 497, 967
Sánchez Almeida, J. 2001, ApJ, 556, 928
Sánchez Almeida, J. 2004, astro-ph/0811.4319

Sánchez Almeida, J. 2005, ApJ, 622, 1292
Sánchez Almeida, J. 2006, in Solar Polarization 4, eds. R. Casini & B. W. Lites, ASP Conf. Ser., 358, ASP, San Francisco, 13
Sánchez Almeida, J., Landi Degl'Innocenti, E., Martínez Pillet, V., Lites, B. W. 1996, ApJ, 466, 537
Sánchez Almeida, J. Lites, B. W. 1992, ApJ, 398, 359
Sánchez Almeida, J., Márquez, I., Bonet, J. A., Domínguez Cerdeña, I. 2007, ApJ, 658, 1357
Sánchez Almeida, J., Martínez Pillet, V., Trujillo Bueno, J., Lites, B. W. 1993, in The Magnetic and Velocity Fields of Solar Active Regions, eds. H. Zirin, G. Ai, & H. Wang, ASP Conf. Ser., 46, ASP, San Francisco, 192
Scharmer, G. B., Gudiksen, B. V., Kiselman, D., Löfdahl, M. G., Rouppe van der Voort, L. H. M. 2002, Nat, 420, 151
Schlichenmaier, R. 2002, Astron. Nachr., 323, 303
Schlichenmaier, R., Bruls, J. H. M. J., Schüssler, M. 1999, A&A, 349, 961
Schlichenmaier, R. Schmidt, W. 2000, A&A, 358, 1122
Schmidt, H. U. 1991, Geophys. Astrophys. Fluid Dyn., 62, 249
Schmidt, H. U., Spruit, H. C., Weiss, N. O. 1986, A&A, 158, 351
Schmidt, W. Fritz, G. 2004, A&A, 421, 735
Schmidt, W. Schlichenmaier, R. 2000, A&A, 364, 829
Sheeley, N. R. 1972, Solar Phys., 25, 98
Solanki, S. K. 2003, A&A Rev., 11, 153
Solanki, S. K. Montavon, C. A. P. 1993, A&A, 275, 283
Spruit, H. C. 1976, Solar Phys., 50, 269
Spruit, H. C. 1987, in The Role of Fine-Scale Magnetic Fields on the Structure of the Solar Atmosphere, eds. E.-H. Schrö ter, M. Váquez, & A. A. Wyller, Cambridge University Press, Cambridge, 199
Spruit, H. C. Scharmer, G. B. 2006, A&A, 447, 343
Stanchfield, D. C. H., Thomas, J. H., Lites, B. W. 1997, ApJ, 477, 485
Stein, R. F. Nordlund, Å. 1998, ApJ, 499, 914
Stix, M. 1991, The Sun (Berlin: Springer-Verlag)
Thomas, J. H. Montesinos, B. 1993, ApJ, 407, 398
Thomas, J. H. Weiss, N. O. 1992, in Sunspots. Theory and Observations, eds. J. H. Thomas & N. O. Weiss, NATO ASI Ser., 375, Kluwer, Dordrecht, 3
Thomas, J. H. Weiss, N. O. 2004, ARA&A, 42, 517
Title, A. M., Frank, Z. A., Shine, R. A., et al. 1993, ApJ, 403, 780
Tritschler, A., Schlichenmaier, R., Bellot Rubio, L. R., the KAOS Team. 2004, A&A, 415, 717
Weiss, N. O., Thomas, J. H., Brummell, N. H., Tobias, S. M. 2004, ApJ, 600, 1073
Zakharov, V., Hirzberger, J., Riethmüller, T. L., Solanki, S. K., Kobel, P. 2008, A&A, 488, L17